

THE ROLE OF ADSORBATES ON FIELD EMISSION

A thesis submitted in partial fulfillment of the requirement  
for the concentration of Physics with Honors  
from the College of William and Mary in Virginia,

by

Justin C. Miller

Accepted for \_\_\_\_\_  
(Honors, High Honors, or Highest Honors)

---

Dr. Keith Griffioen

---

Dr. Roy Champion, Honors Advisor

---

Dr. Dennis Manos

---

Dr. James E. Smith

Williamsburg, Virginia

April 2002

## I. Abstract

Experimental studies of the effects of various gas adsorbates on the emission characteristics of Spindt-type molybdenum field emission cathode arrays [1] have been performed. Sputter cleaning with an argon-ion ( $\text{Ar}^+$ ) beam was used in an attempt to remove adsorbed molecules from the surface of the field emitter (i.e., the molybdenum tips). It was anticipated that surface alteration by way of adsorbate removal would alter the emission characteristics, possibly reducing field emission. The reapplication of adsorbate to a sputter-cleaned surface was precisely controlled with the gas-handling system. It was our goal to correlate the field emission with the amount of adsorbate on the surface and compare the results with that predicted for field emission from an adsorbate-free surface as described in the seminal work of Fowler and Nordheim [2].

The sputter-cleaning scheme consisted of directing a 1 nanoampere  $\text{Ar}^+$  ion beam to the tips for one hour. Such cleaning invariably reduced field emission. Adsorbates were then reintroduced to the surface in an attempt to “restore” the emission. Of the adsorbates studied, none appeared to clearly and consistently return the emission of the field emitter array to the pre-cleaning levels. Instead, the only way to return field emission back to baseline levels was to let the emitter relax for a period of about twenty-four hours. A slow thermal diffusion process is proposed to account for the steady increase in field emission after cleaning.

## II. Introduction

Through the use of thin-film technology and electron beam microlithography, Dr. Capp Spindt and his co-workers at the Stanford Research Institute (SRI International) have fabricated molybdenum cones as field emission cathodes for several decades [1]. This technique has been refined to produce field emitter arrays (FEAs) with large numbers of cones regularly packed into a small area. Field emitter array technologies have been pursued in the display industry as a more efficient alternative to cathode ray tubes and liquid-crystal displays (LCDs) [3]. The field emitter technology could conceivably run at lower power than current LCDs and at a thinner depth than current flat-panel technology [1].

The Spindt-type field emission cathodes' geometry is partially responsible for its remarkable field emission properties. As illustrated schematically in Figure 1, the

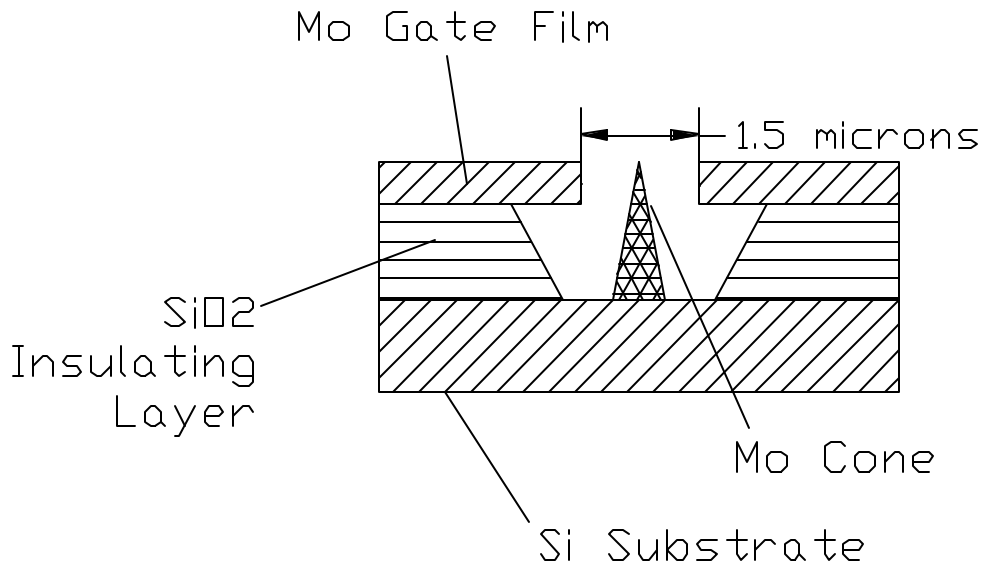


FIG. 1. Schematic diagram of a typical Spindt-type field emission cathode

cathode structure consists of a molybdenum cone surrounded by a molybdenum gate film on top of a  $\text{SiO}_2$  insulating layer. The cones/tips are exposed via holes in the gate on the order of  $1.5 \mu\text{m}$  in diameter. The tips and gate structure sit on a silicon substrate. This configuration is the conductor – insulator – conductor sandwich required for field emission properties. Tips of various heights, sizes, and array densities are manufactured to create field emitters with distinct properties [1].

The low-voltage operation of Spindt-type FEAs provides several advantages over previously used field emitters. Functioning at a much lower voltage than etched wire emitters exposes the FEAs to much lower risk of damage from the ionization of ambient gas inside the vacuum chamber [4]. This property allows for operation at much higher pressure with a longer operating lifetime than older emitter technologies. In addition, the FEAs have an actual current density per useful lifetime much greater than thermionic cathodes [5].

Thermionic or thermal-emission cathodes describe electron emission for situations where cathode temperature is high and relative field strength is low [6]. Figure 2 displays the typical potential energy diagram for the free-electron gas model of conduction in a metal. As the temperature of a metal increases, the electron states within the metal surface become more and more smeared out around the Fermi level ( $e_f$ ) of the metal. The occupation of states above the Fermi energy is of particular interest. In the diagram,  $f$  is the work function of the metal,  $e$  is the energy level of a particular electron, and  $e = 0$  is the ground state electron in the surface. At a high enough temperature, the highest electron energy levels exceed the barrier potential that retains them within the surface. The electrons can then escape the surface of the metal into the vacuum resulting

in thermionic emission. Thermionic emission is commonly used in cathode ray tubes where a tungsten filament at several thousand Kelvin is held at a lower potential than the anode. As electrons escape the filament, they are guided to the phosphorescent anode with various steering potentials. This technology is the basis for most television sets and CRT monitors.

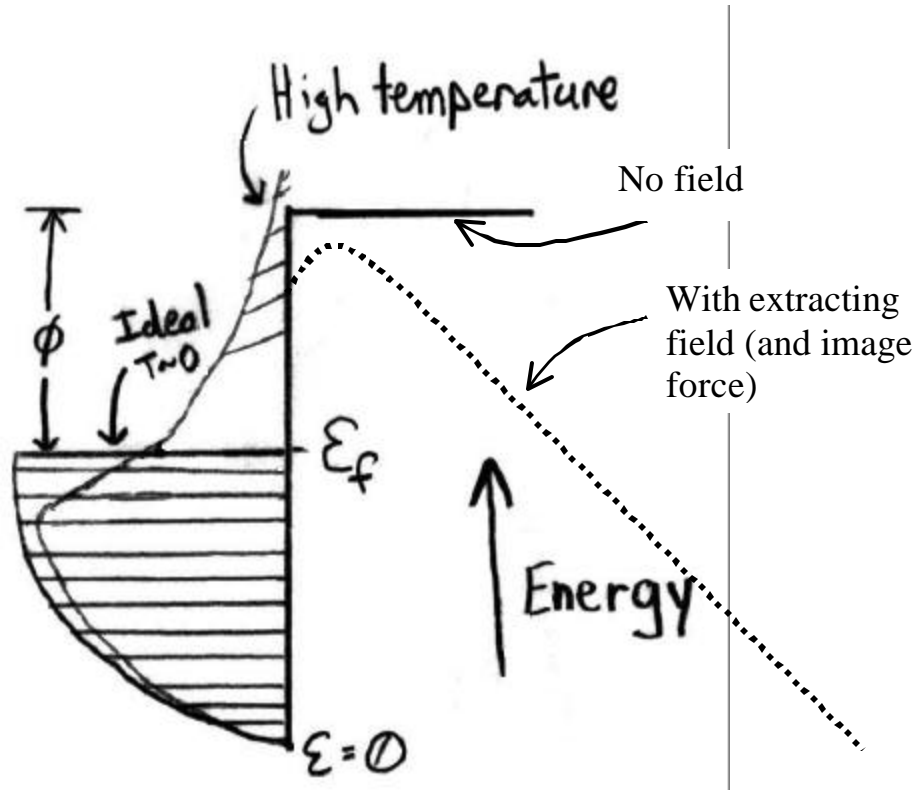


FIG. 2. Energy diagram for thermionic electron emission

Fowler-Nordheim theory explains the cold cathode field emission at low temperatures in regions of high electric fields [1,6]. The resulting Fowler-Nordheim relationship between emitted current and extraction field is a fair prediction of current density for FEAs [1,2]. The familiar relation is used to correlate field emission current,  $J$ , in Amperes per square centimeter to the electric field at the surface,  $E$ , in volts per centimeter and the work function  $f$  in electron volts by

$$J = \frac{AE^2}{\mathbf{f}t^2(y)} \exp\left(-B \frac{\mathbf{f}^{3/2}}{E} v(y)\right), \quad (1)$$

where

$$A = 1.54 \times 10^{-6} \frac{\text{eV}}{\text{V}^2}, \quad (2)$$

$$B = 6.87 \times 10^7 \frac{\text{V}}{\text{cm} \cdot \text{eV}^{3/2}}, \quad (3)$$

and  $y$  is the Schottky lowering of the work-function barrier. The image forces experienced by a charged particle near a metal surface cause this barrier to lower and to curve. Here,  $A$  and  $B$  are coefficients which depend upon the units of  $E$  and  $\mathbf{f}$  forcing the term in the exponential to be unitless and the overall value of Equation 1 to be in units of field emission current. In Equation 1,  $t(y)$  and  $v(y)$  are unitless elliptic functions which have been approximated by Spindt [1] as

$$t(y) = 1.1 \quad (4)$$

and

$$v(y) = 0.95 - y^2 \quad (5).$$

The function  $v(y)$  takes into account the image force experienced by the electron at the field-emitter surface, and  $t(y)$  is nearly unity [7]. Values for  $v(y)$ ,  $t(y)$ , and  $y$  have been tabulated based on corrections to the previous work of Nordheim [8, 9]. The usual Fowler-Nordheim relation can be obtained from Equation 1 by noting that

$$J = I / \mathbf{a}, \quad (6)$$

$$E = \mathbf{b}V / d, \quad (7)$$

where  $I$  is the field emission current in Amperes,  $V$  is the applied voltage in volts,  $\mathbf{a}$  is the emitting area in square centimeters,  $\mathbf{b}$  is a unitless field enhancement factor owing to the geometry of the actual tip structure, and  $d$  is the gap dimension in centimeters. The sharpness of the points obviously dictates the value of  $\mathbf{b}$  and is often as large as a few hundred (e.g., the field at a surface with a small radius of curvature can be much larger than  $V/d$ ). Hence, simple substitution of Equations 6 and 7 into Equation 1 yields

$$\frac{I}{\mathbf{a}} = \frac{A(\mathbf{b}V/d)^2}{\mathbf{f}t^2(y)} \exp\left(-B \frac{\mathbf{f}^{3/2}}{\mathbf{b}V/d} v(y)\right). \quad (8)$$

Finally, rearrangement and redefining the coefficients yields

$$I = aV^2 \exp\left(-\frac{b}{V}\right) \quad (9)$$

where

$$a = \frac{\mathbf{a}A\mathbf{b}^2}{1.1\mathbf{f}d^2} \exp\left(\frac{B(1.44 \times 10^{-7})d}{\mathbf{f}^{1/2}}\right) \quad \text{and} \quad (10)$$

$$b = \frac{0.95B\mathbf{f}^{3/2}}{\mathbf{b}} \quad (11).$$

Again,  $A$ ,  $B$ ,  $\mathbf{f}$ , and  $d$  are scalar values;  $a$  depends primarily on the emitting surface area and  $b$  depends on the shape and radius of the tips [1]. Rearranging Equation 9 produces

$$\ln\left(\frac{I}{a \cdot V^2}\right) = -\frac{b}{V} \quad (12)$$

which is the familiar linear relationship between the natural logarithm of  $(I/V^2)$  versus  $1/V$ . In Figure 3, this familiar relationship between the natural log of  $I$  over  $V^2$  versus the inverse of  $V$  is displayed for the first field emitter array that was used in the present experiments. Note that the Fowler-Nordheim calculation yields the straight line while the

experimental data diverges from that predicted by the relatively simple model at the extremes of its operation (i.e., where the FEA just begins to emit and at the high end of field emission).

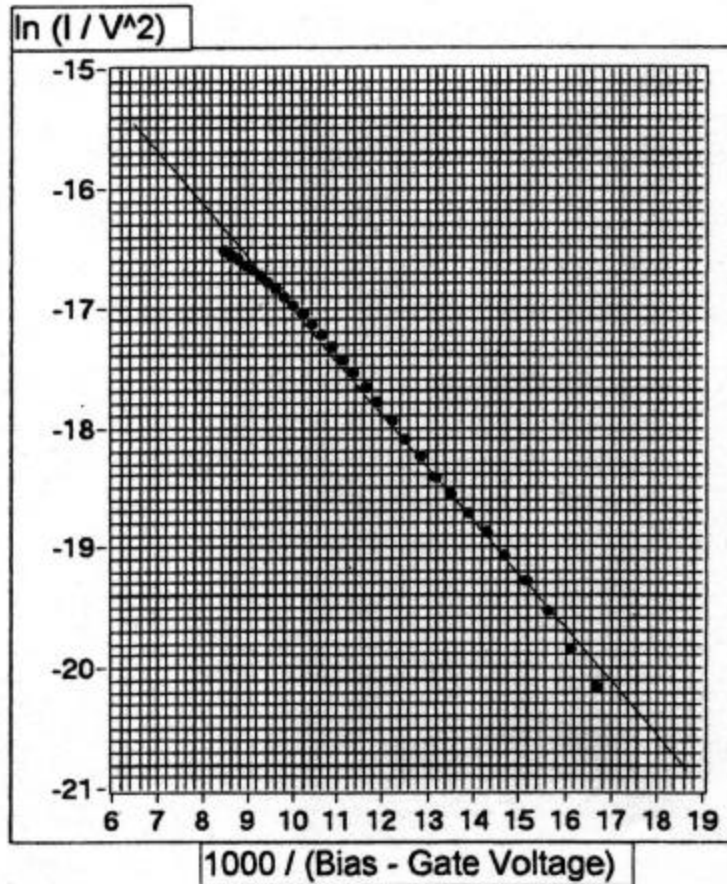


FIG. 3. Fowler-Nordheim plot for our FEA, courtesy of SRI International Cathode Information Sheet

Field emission from the structure is not completely understood if one assumes a smooth, spherical cap structure at the tip of the cones. In fact, the field emission is observed to exceed that which would be anticipated without including an additional emission enhancement factor [1]. Surface adsorbates have been suggested as the reason for this enhanced emission [1]. Because of the very sensitive nature of the molybdenum gates and tips, the cathodes cannot simply be heated to temperatures necessary to completely remove adsorbed and dissolved gases from the emitting area.

The adsorption of oxygen onto molybdenum has been summarized previously [10]. Oxygen molecules dissociatively adsorb onto the surface of molybdenum because the binding energy between oxygen and molybdenum is greater than the binding energy between two oxygen atoms in an O<sub>2</sub> molecule [11, 12]. Moreover, the adsorbed oxygen acquires an “extra” electron and resides on the surface as O<sup>-</sup>.

The gas exposure is a measure of the amount of gas to which a surface has been subjected and, depending upon the probability of sticking to the surface, determines the degree of adsorbate coverage on a surface. The unit of gas exposure is the Langmuir and is equivalent to 10<sup>-6</sup> Torr-seconds of exposure. If all impinging molecules stuck to the surface, one Langmuir would result in roughly one monolayer of coverage. For example, one monolayer of oxygen adsorbate on Mo(100) follows its exposure to around 10 Langmuir of O<sub>2</sub> [11]. Previous investigations have indicated that adsorbed gases can vastly alter the emission characteristics for massive exposure [13-17]. However, these studies have not clearly described any cleaning measures undertaken to free the surface of adsorbates prior to gas exposure [15-17].

Due to the highly sensitive nature of the tips, research to date does not appear to involve proper removal of adsorbed gas from the surface. When determining the effects of gas exposure on emission properties, it seems that residual adsorbates have not been removed. This could easily confound results for low gas concentrations on the surface. It appears that the true emission characteristics of the field emitter array (i.e., where the array is clear of adsorbates) have not been studied. It is the goal of this inquiry to determine what effect adsorbates, especially oxygen (O<sub>2</sub>), have on the emission

characteristics of Spindt-type field emitter arrays by cleaning adsorbates from and reintroducing adsorbates to the surface.

### **III. Theory**

The Fowler-Nordheim relation treats a cold cathode electron emission from a clean metal surface as simple barrier penetration. When sufficiently large electrostatic fields are applied to a cold cathode, electrons can quantum-mechanically tunnel from the metal through the classically forbidden region out of the metal [2]. Fowler and Nordheim originally considered the problem of a triangle barrier and then the triangle barrier rounded by the image potential experienced by the tunneling electron.

Figure 4 depicts the result of Fowler and Nordheim's treatment of an electron tunneling from the potential of a metal surface. The diagram depicts the original triangle barrier potential (heavy dotted lines) where only an electric field has modified the square potential. The image force experienced by the electron as it escapes from the surface is shown in the short-dotted line. Combining these factors together produces the rounded triangle barrier potential which Fowler and Nordheim studied.

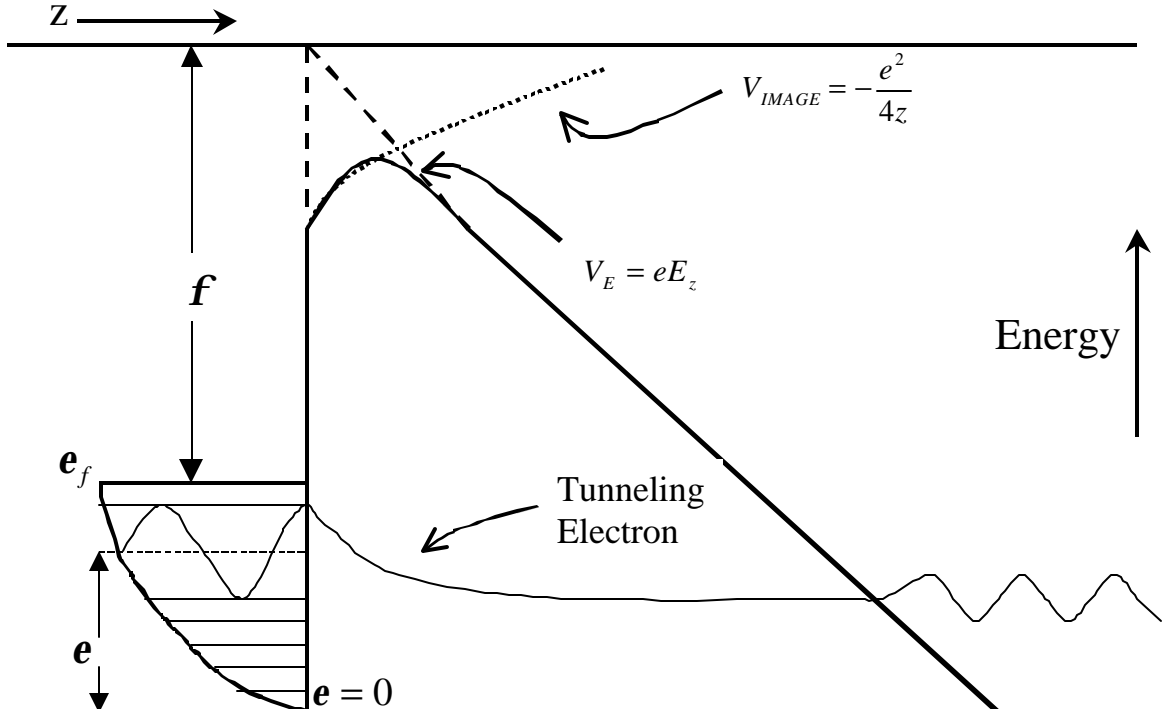


FIG. 4 Field emission via tunneling through an idealized potential

They found the exact solution to the triangular barrier problem in which the surface potential is taken as a step function plus the applied field. The oscillating wave function solutions are characterized by a “wave number,”  $k$ . For the region where the electron is tunneling through the barrier,  $k$  is imaginary, signifying exponential decay. For all other regions,  $k$  is pure real, indicating an oscillating wave traveling out from the surface. Gadzuk describes how this exact solution can be found and subsequently analyzed through several approximations and simplifications [18]. However, a numerical approximation is necessary to get a functional result. The result for the transmission probability,  $D_m$ , as a function of normal energy,  $W$ , is given by

$$D_m(W) \cong \exp \left\{ -c_0 + \left[ \frac{(W - e_F)}{d_0} \right] \right\}, \quad (13)$$

where  $e_F$  is the fermi energy level in electron volts and

$$c_0 = \left( 0.683 \frac{V}{eV^{3/2} \cdot \text{\AA}} \right) \cdot \frac{f^{3/2}}{E}, \quad (14)$$

$$\frac{1}{d_0} = \left[ \left( 1.025 \frac{V}{eV^{1/2} \cdot \text{\AA}} \right) \cdot \frac{f^{1/2}}{E} \right] eV^{-1}, \quad (15)$$

$$W = e + V_0 - \left( \frac{\eta^2}{2m} \right) k_t^2, \quad (16)$$

$$V_0 = e_F + f, \quad (17)$$

when  $f$  is in electron volts,  $E$  is in volts per angstrom,  $e$  is the energy level of the electron,  $m$  is the mass of the electron,  $k_t$  is the wave number, and  $\eta$  is Planck's constant divided by  $2\pi$ . The fundamentally exponential behavior of the dependence is the notable result of this analysis. This analysis is only possible because the Schrödinger equation for this potential can be reduced to one of the standard equations in mathematical physics.

Approximation schemes permit additional analysis of the electron wave function. In cases where an exact solution to the Schrödinger equation cannot be found, approximations are the only way to analyze the potential to determine transmission behavior. Gadzuk employs the Wentzel-Kramers-Brillouin (WKB) approximation and further refines it with the work of Miller and Good [18]. The WKB approximation is valid as long as the spatial variation of the potential is small over an electron wavelength in the classically allowed region or over a characteristic decay length in the classically forbidden region. The result of the WKB approximation is

$$D_{WKB}(W) \cong \exp \left\{ -c + \left[ \frac{(W - e_F)}{d} \right] \right\}, \quad (18)$$

where

$$c = c_0 \cdot v \left( \left[ 3.79eV \cdot \sqrt{\frac{\overset{\circ}{\text{A}}}{\text{V}}} \right] \frac{E^{1/2}}{\mathbf{f}} \right) \quad (19)$$

$$\frac{1}{d} = \frac{1}{d_0} \cdot t \left( \left[ 3.79eV \cdot \sqrt{\frac{\overset{\circ}{\text{A}}}{\text{V}}} \right] \frac{E^{1/2}}{\mathbf{f}} \right) \quad (20)$$

with  $v(y)$  and  $t(y)$  as the elliptic functions described above and tabulated previously [18].

The additional elliptic terms are the only modifications to the tunneling probability, which remains basically exponential as before. The Miller-Good approximation corrects the WKB transmission function for some functional behavior that is incorrect near the classical turning points (i.e., near the barrier as  $k \approx 0$ ). Additional corrections may also be necessary for situations where low-field thermionic emission occurs [18].

However, the presence of adsorbates will clearly alter the potential experienced by the tunneling electrons. Adsorbed oxygen on the surface of the molybdenum will reside as  $\text{O}^-$ , as the image-shifted electron affinity of oxygen will lie below  $\mathbf{e}_f$ . In the potential energy diagram of Figure 5, distance from the metal surface is shown by the  $z$ -axis. The molecule adsorbed on the surface may create a potential well at a certain distance,  $z_{eq}$ . This could cause the emission properties of the molybdenum to be considerably different for a surface free of adsorbate, as the emitted electron may arise from the  $\text{O}^-$  potential well where the tunnel barrier is less than that depicted in Figure 4.

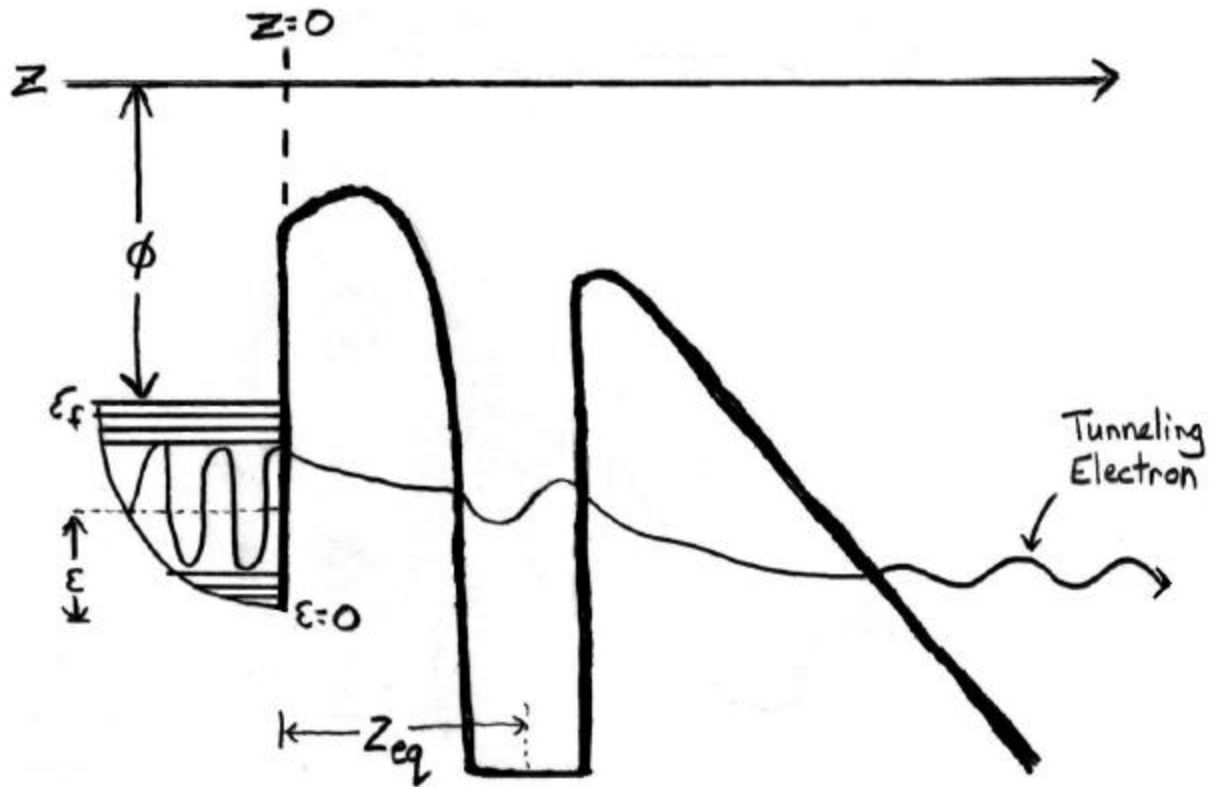


FIG. 5. Schematic diagram of the electron “pseudopotential” describing field emission in the presence of an adsorbed atom

Accordingly such tunneling should be completely different from that described by field emission from a free-electron gas model of a metal [14, 15]. Consequently, the tunneling probability and the field emission may strongly depend upon the oxygen or other gas adsorption on the molybdenum tips. This potential well from the adsorbed molecule has been postulated to alter a factor in the WKB approximation, increasing the transmission probability of the electron [18]. It was our hope that the experimental data might be compared with this altered barrier potential.

## IV. Experiment

The experimental chamber is an ultrahigh vacuum apparatus operating at a base pressure below  $2 \times 10^{-9}$  Torr following a 12 hour system bakeout at 200 °C. Experiments must be conducted in an ultrahigh vacuum for a variety of reasons. A vacuum is necessary for atomically cleaning surfaces for study, and for such surfaces to be maintained in a contamination-free state for the duration of the experiment. Furthermore, control of adsorbed gases onto a metal surface is only possible in a vacuum environment. A vacuum allows the use of low energy electron and ion-based technologies without scattering interference from the surrounding gas molecules. Lastly, operation of this particular field emitter array is only possible in an ultrahigh vacuum environment.

As in Figure 6, the cathode is an array, with an active area of  $\sim 1\text{mm}^2$ , with 10,000 to 50,000 Spindt-type molybdenum tips. The assembly is mounted on a T0-5 header. The first two field emitters that were used in the present experiments had only 10,000 tips. The third and fourth cathodes had 50,000 tips, and the fourth was used primarily for the adsorbate-related trials. The first three failed catastrophically during the refinement of experimental methods (see Results for discussion of the failures). During cathode operation, the gate voltage was kept at a constant +20 volts while the voltage to the tips was varied from 0 to -80 volts relative to the gate with different steps depending on the region of interest. There was a ten to twenty second delay per step to allow the field emission to stabilize before the collector current and tip-gate voltage was recorded. The gate and tip voltages are controlled via the LabView computer program with a Kepco programmable power supply and measured by a Keithly 175 multimeter. For measurement, a 1-inch by 1-inch square collector sits opposite the FEA at a +60 volt bias.

As displayed in Figure 6, the collector is overly large and curved slightly to shield the mounting mechanism from any stray electric fields and improve measurement accuracy. The collector current is amplified by an SRS model SR570 low-noise current preamplifier and measured by a Fluke 45 dual display multimeter. The FEA is mounted on a moveable armature allowing it to face the ion gun for cleaning (horizontal) and to angle down to the collector face at  $45^\circ$  below the horizontal. The armature also permits three translational degrees of freedom and one other rotational degree of freedom. These other degrees of freedom were not changed after the cleaning distance was set.

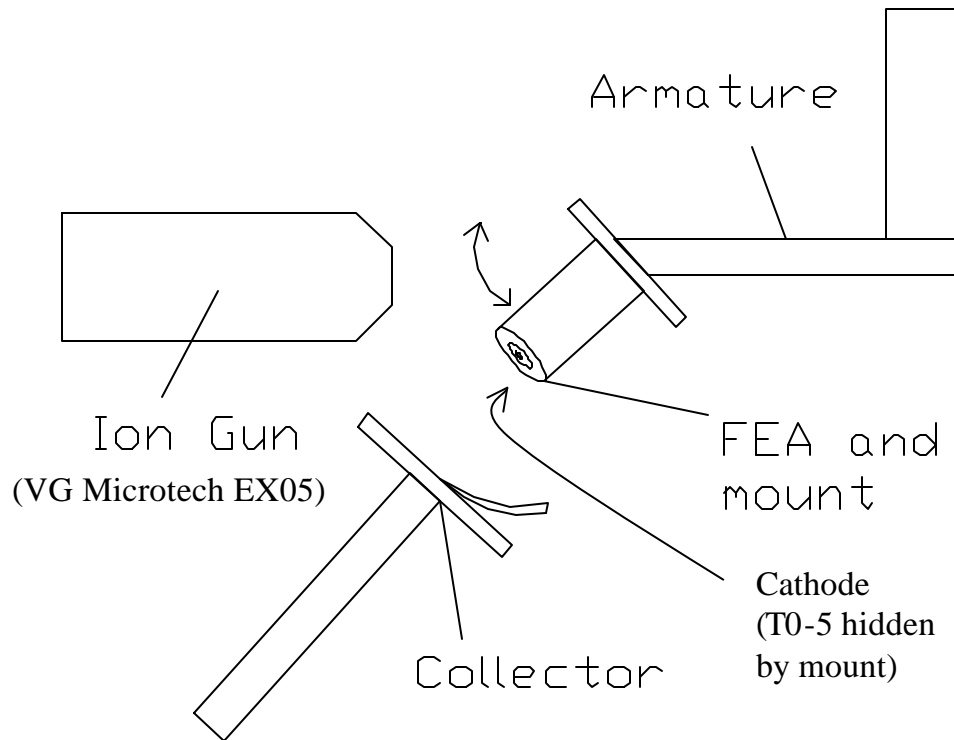


FIG. 6. Experimental apparatus, side-view

For cleaning, a VG Microtech EX05 ion gun is employed to bombard the array surface with argon ions ( $\text{Ar}^+$ ) at energies ranging from 100 eV to 2 keV. The tip current

(and in later trials the gate current) was amplified by the SRS model SR570 low-noise current preamplifier and measured by a Fluke 45 dual display multimeter. A current of 1 nanoampere (nA) at the tips (3.5 – 4.0 nA at the gate in later trials) was determined to be optimal in terms of feasibility, measurability, and efficacy without risking damage to the FEA.

A cleaning time of one hour was determined such that the number of ions striking each square angstrom of emitter surface would be on the order of unity. The following calculations are for the 50,000 tip FEAs used for much of the adsorbate study. Based upon electron micrograph scans of the FEA, the measurements found in Table 1 were made. The distance between the centers of two adjacent tips was determined to be 3.5 microns. Because the tips are arranged in a square grid, dividing the total emitting area by the square of the inter-tip distance (the area of one tip and surrounding gate material)

Object	Diameter of base ( $\mu\text{m}$ )	Area ( $\mu\text{m}^2$ )
One Tip	2.2	3.80
Active Cathode Area (all tips and gates)	900	636,173

Table 1. FEA measurements from SEM photographs

yields an approximation of the number of tips in the FEA. This approximation of 52,000 tips agrees with the supplied data sheet stating that there are approximately 50,000 tips in that particular FEA. The desired current at the tips is 1 nA, which corresponds to  $10^{-9}$  Coulombs per second. Each argon ion carries the fundamental charge of  $1.6 \times 10^{-19}$  Coulombs because each is deficient by one electron. The total area of the tips would be 50,000 times  $3.80 \mu\text{m}^2$ . It should be noted that the spot size of the ion beam is

approximately the same as the size of the emitting area and the two are assumed to be equal for the purpose of this calculation. This is not an unreasonable assumption based upon the characteristics of this particular ion gun. The flux at the tips would be:

$$10^{-9} \frac{C}{s} \cdot \frac{1 \text{ electron}}{1.6 \times 10^{-19} C} \cdot \frac{1}{50,000 \cdot 3.80 \text{mm}^2 \cdot 10^8 \text{A}^2 / \text{mm}^2} = 0.000329 \frac{\text{incident ions}}{s \cdot \text{A}^2}. \quad (21)$$

This corresponds to ~3000 seconds (51 minutes) for one ion to impact each square angstrom. Since the desired ion impact for each square angstrom is desired to be on the order of unity, the cleaning time of one hour at 1 nA of current to the tips is reasonable.

Initial tests of the field emitter array concerned the determination of whether cleaning with the argon-ion beam was feasible without damaging the surface and if so, what beam energy is safe and effective. The optimum beam energy for cleaning without causing damage to the tips was experimentally determined. The incident ion energy was slowly increased from 100 eV up to approximately 1.125 keV in steps of 100 eV per trial. At the 1 keV level, emission was observed to clearly decrease after successive cleaning runs and return to baseline emission slowly.

Significant care has been taken to prevent any damage to the field emitter array during cleaning and regular operation. One reason for the lack of research concerning adsorbed gases is the acute sensitivity of the molybdenum tips to disruption and damage. Figure 7 depicts some of the early data taken to determine the proper interval of cleaning. The field emission from 30 – 45 V is reduced with additional cleaning. Additional trials have corroborated the reduction in field emission as cleaning time increased up to a certain level. Much time has been spent to establish a feasible operating range with which to sputter adsorbed molecules from the tips without adversely affecting the tip

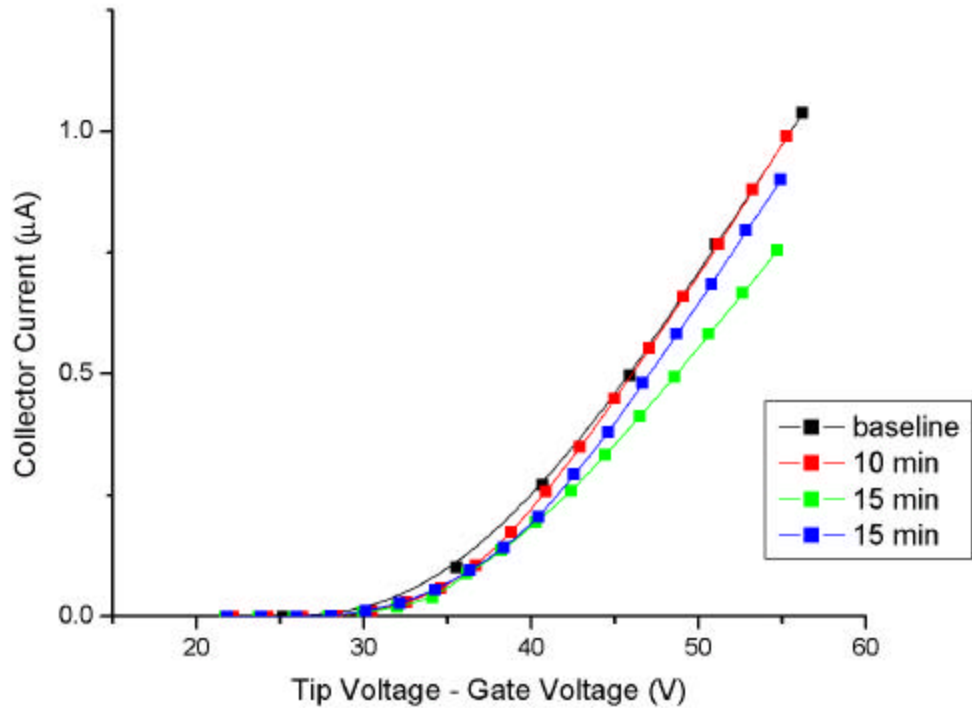


FIG. 7. Voltage versus Collector Current for Various Ar<sup>+</sup> cleaning times at 450 eV (First FEA)

geometry. In our initial tests, emission performance appeared to improve slightly after some argon ion bombardment. Then performance shifted back to baseline levels in the presence of additional ion bombardment.

Further investigation showed that the initial cleaning intensity was not sufficient. The desired current at the field-emitter tips of 1 nA was sufficient. However, configuration of the cathode confounded the measurement of this value. Because portions of the tip header were exposed to the ion beam during cleaning, it was possible to measure 1 nA of current to the structure electrically connected to the cathode without actually delivering that current to the emitter portion of the structure. The beam was also impacting the other exposed portions of the header on which the tips were mounted. Once this fact was realized, gate current was monitored during cleaning such that 1 nA

was guaranteed at the tips based upon relative area and flux calculations. With this new cleaning scheme, emission clearly decreased immediately after cleaning. The emission was observed to slowly return over the course of twelve hours, rising without exception to baseline levels within twenty-four hours. Because the emission clearly declined upon argon-ion beam bombardment, argon-ion cleaning was apparently modifying the nature of the adsorbate density. Since the emission always returned to baseline levels the morning following cleaning, it seems clear that systematic destruction of the field-emitter did not occur.

After a safe operating range was determined for the FEA, a gas-handling system was added in order to precisely control the reintroduction of adsorbates. Initially, the effect of adsorbed oxygen was tested via exposure through a Granville-Philips Co. precision leak valve with the partial pressure measured by a Granville-Philips Co. vacuum controller reading a Varian nude Bayard-Alpert type ionization gauge. With the gas handling system, adsorbate can be added back via the leak valve after being sputter-cleaned from the surface via the argon ion beam. We anticipated studying shifts in the relationship between collector current and tip-gate voltage as a result of varying adsorbate coverage.

## **V. Method**

When taking an I-versus-V data set, the cathode was aligned perpendicular to the collector plate using the movable armature. The collector plate was biased at +60 volts in order to effectively collect the emitted electrons. The gate was biased at +20 volts relative to the tips. Several values were set in the Labview computer program based on

the data set and test desired. These included the maximum voltage difference between the tips and gates (less the initial +20 volt gate bias), the step in voltage for each datum, and the interval between changing the voltage and measuring each datum to allow the field emission to stabilize. Data was then imported from the Labview program into the Origin software graphing package for further analysis.

When exposing the field emitter array to an adsorbate, significant care was taken to avoid damage to the FEA. The adsorbate gas was released into the main chamber from a two-stage gas-handling system. Stage one was connected to stage two which was connected to the main chamber. Stages one and two were isolated from each other via a gate valve. Stage two was separated from the main chamber via a precision leak valve. All valves separating the system were normally closed except when filling stage two or releasing adsorbate into the main chamber. The adsorbate gas was stored in a lecture bottle in stage one of the gas-handling system. When exposing to adsorbate, stage two was first filled with gas from stage one via the gate valve and measured with a pressure gauge. Then the gate valve separating stages one and two was closed. Desired exposure levels were used to calculate the exposure time at a specific pressure. The desired pressure was monitored in the main chamber using the ion gauge while gas was released from stage two into the main chamber via the precision leak valve for the desired time. During exposure, the gate, tips, and collector were all separated from their respective power supplies and grounded to prevent damage due to arcing as the chamber reached higher pressures. The precise identity of the adsorbate species released could be double-checked via a UTI Model 100C precision residual gas analyzer (also mass spectrometer or RGA) and displayed on a Tektronix type RM 564 storage oscilloscope after data had

been taken. Because the ion gun in the mass spectrometer released many electrons into the main chamber during operation, it could not be operated at the same time as field emission experiments without interfering with the measurements. This RGA measurement provided further assurance that contaminants had not entered the system and that leaks were not confounding the experiment.

## **VI. Results**

Early trials involved the refinement of experimental techniques with regard to cleaning energies and determination of an acceptable gate-tip voltage range for field emission. During these early trials, cleaning was ineffective because the current measured at the tips was not correct due to the aforementioned exposed tip electrode. Thus field emission did not appear to change appreciably when cleaning and exposure as in Figures 8a and 8b. The cleaning energy for this trial was 1 keV. These trials were conducted using the fourth cathode, which tended to be much more efficient than the previous three. The current measured at the collector was on the order of milliamperes as opposed to microamperes in Figure 7. With five times as many tips as each of the first two cathodes, this cathode was much more efficient when emitting.

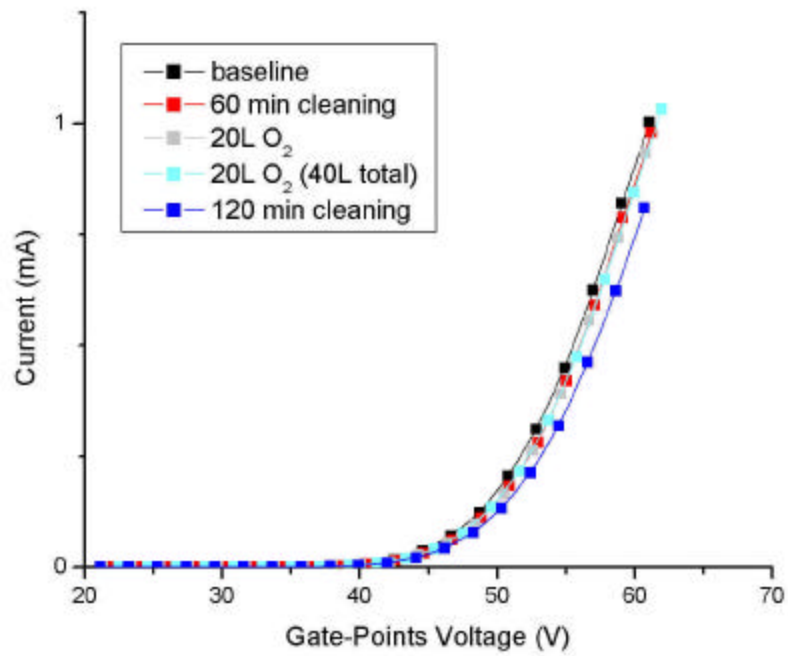


FIG. 8a. Voltage versus Collector Current for  $\text{Ar}^+$  cleaning 1 keV (Cleaning inadequate)

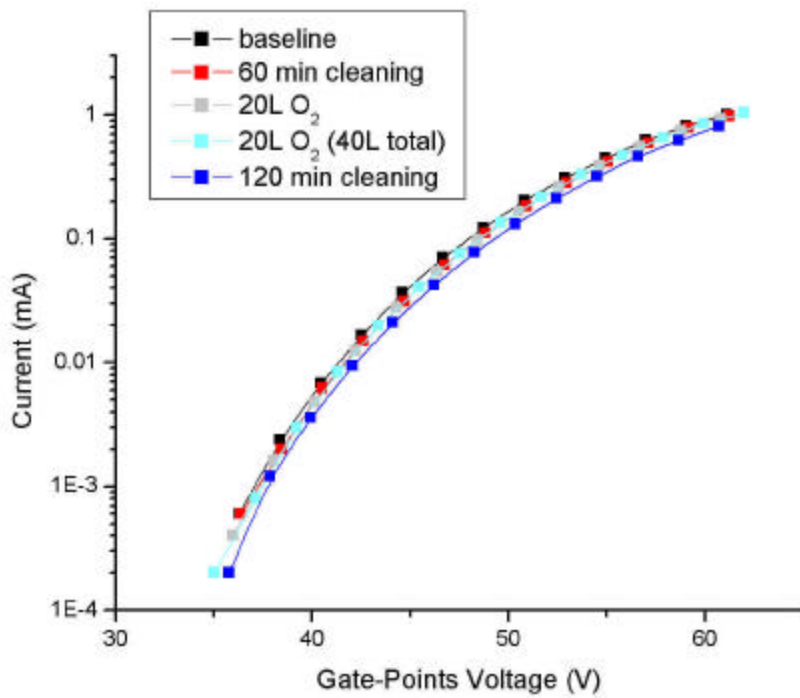


FIG. 8b. Voltage versus Collector Current for  $\text{Ar}^+$  cleaning 1 keV (Cleaning inadequate) Logarithmic Scale

When a new cathode was placed in the chamber, the early trials involving both cleaning and adsorbate exposure tended to improve the emission, as did simply waiting between trials. Note that this was the case in Figures 9a and 9b. Exposure in Figure 9a was limited to oxygen gas. While these figures include many trials, the important observation is that emission remains unchanged or increases for each trial regardless of what is done to the FEA. These initial variations in I versus V were probably caused by the desorption and removal of various hydrocarbons and other contaminants since the cathode had not been “conditioned” after its fabrication and installation process. Removing the contaminating adsorbate species was thought to improve field emission to a point (considered original baseline levels) after which additional cleaning causes decreased emission. If nothing was done to the surface in terms of cleaning and exposure, the emission would slowly increase to the original baseline level over the

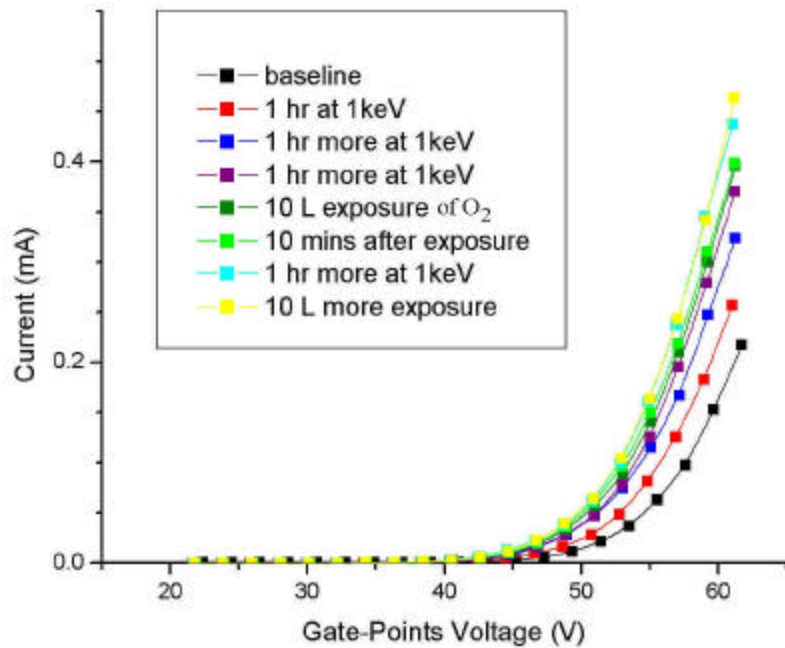


FIG. 9a. Early trial of Voltage versus Collector Current for Ar<sup>+</sup> cleaning 1 keV, Oxygen exposure

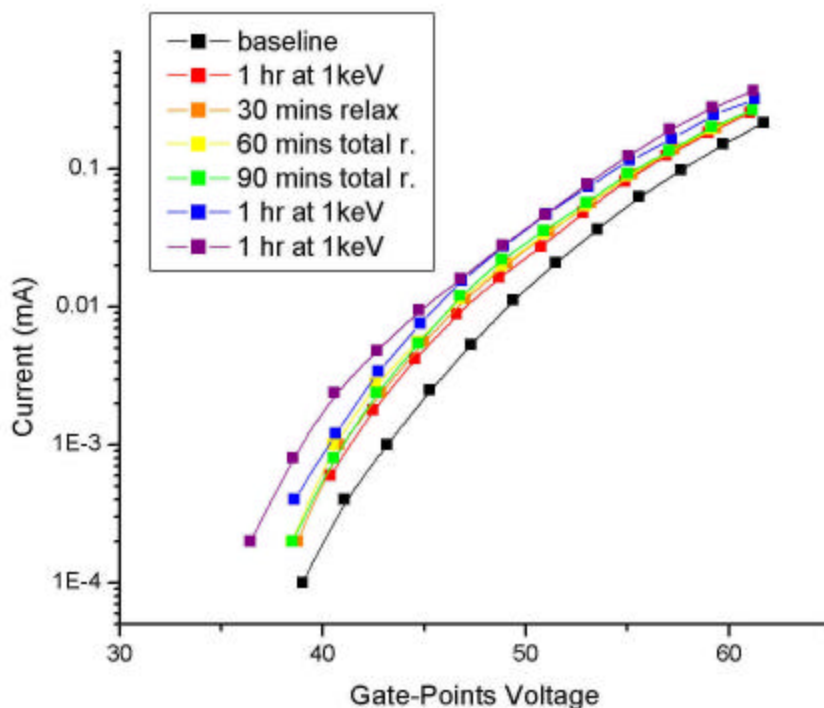


FIG. 9b. Another early trial of Voltage versus Collector Current for  $\text{Ar}^+$  cleaning 1 keV (Logarithmic scale)

course of several hours. The cause of the decline while cleaning is believed to be the removal of specific adsorbate species on the tips, which tends to improve field emission. It has been the goal of this investigation to discover the identity and nature of this adsorbate species. Based upon mass spectrometer measurements of the main chamber contents, trace gases include hydrogen, water, nitrogen, oxygen, and carbon dioxide with water and its ionic radicals being dominant.

Initially, tests focused on oxygen as an adsorbate because its interactions with molybdenum are well understood as previously discussed. Adsorbate species were confirmed at the end of each day using the gas analyzer. When oxygen was applied to a previously cleaned surface as an adsorbate, emission immediately decreased and only returned to previous levels after approximately an hour. This behavior can be observed

in Figures 10a and 10b. After a baseline reading, the surface was cleaned and then exposed to 20L of oxygen. The system was then allowed to “relax” in a background pressure of  $\sim 10^{-9}$  Torr. I-V measurements were then made over time. The gradual progression back to baseline emission can be observed in Figures 10a and 10b. Finally, at 5:30 p.m., the FEA was exposed to 20L more oxygen. Here the immediate decline in emission is evident. Again, emission begins to relax back to baseline levels.

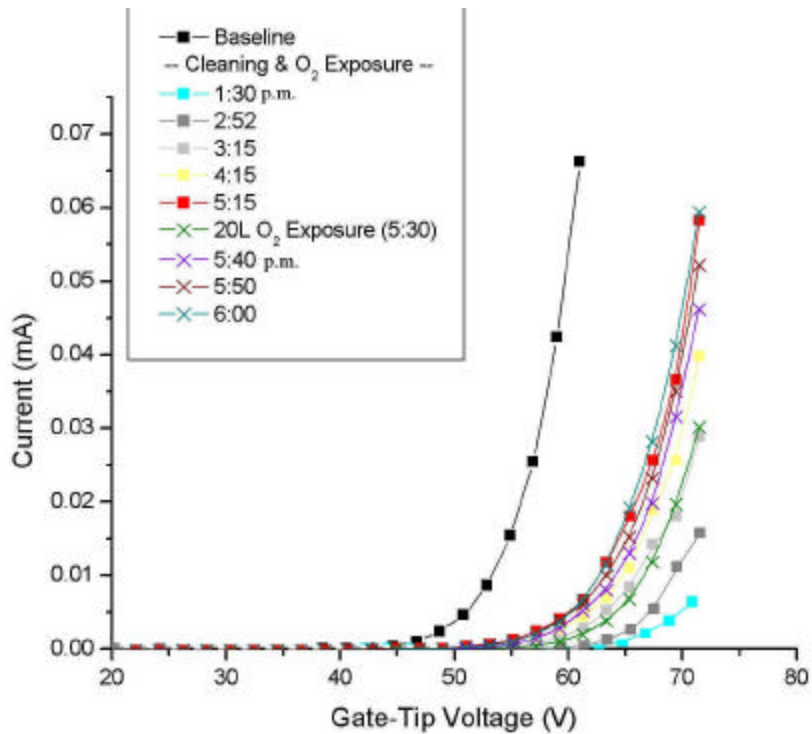


FIG. 10a. Oxygen cleaning & exposure plot of Voltage versus Collector Current for  $\text{Ar}^+$  cleaning 1 keV

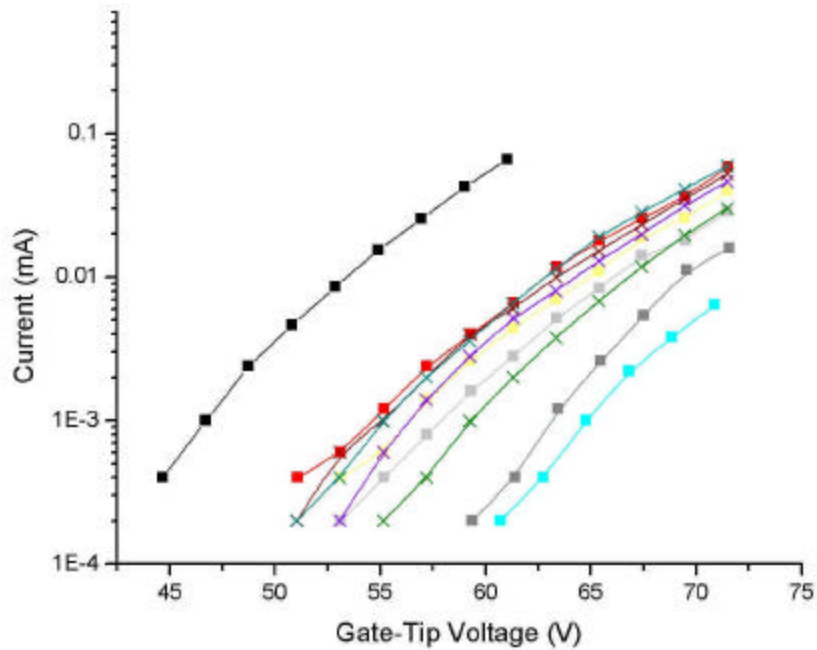


FIG. 10b. Oxygen cleaning & exposure plot of Voltage versus Collector Current for  $\text{Ar}^+$  cleaning 1 keV (Logarithmic scale)

Hydrogen was the next focus of the investigation. At this point, the cleaning and reapplication of adsorbate had become a refined process resulting in much faster trials. Hydrogen was quickly ruled out as the adsorbate responsible for increasing emission. As shown in Figures 11a and 11b, hydrogen application at an exposure large enough to reveal any clear dependence does not immediately impact field emission. In additional trials, repeated hydrogen dosing at both higher and lower concentrations did not appear to alter the field emission beyond the slow increase in emission over time.

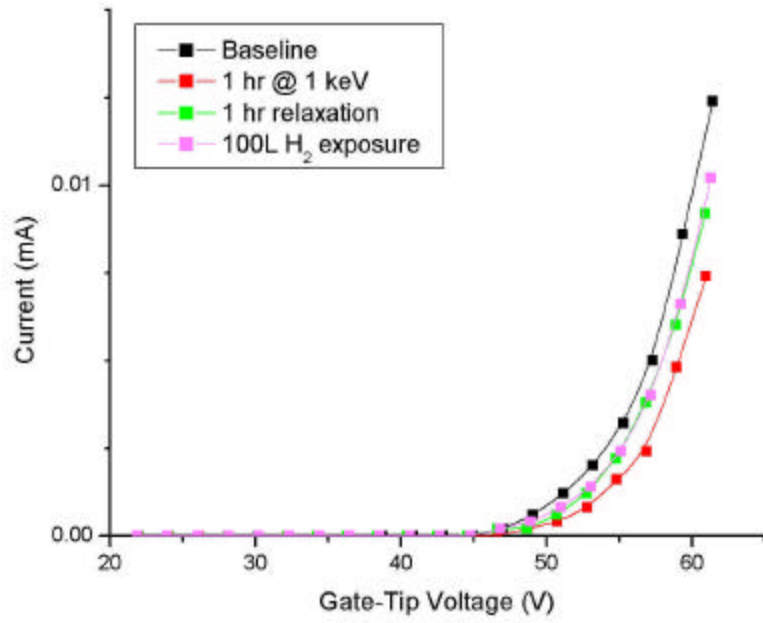


FIG. 11a. Hydrogen cleaning & exposure plot of Voltage versus Collector Current for  $\text{Ar}^+$  cleaning 1 keV

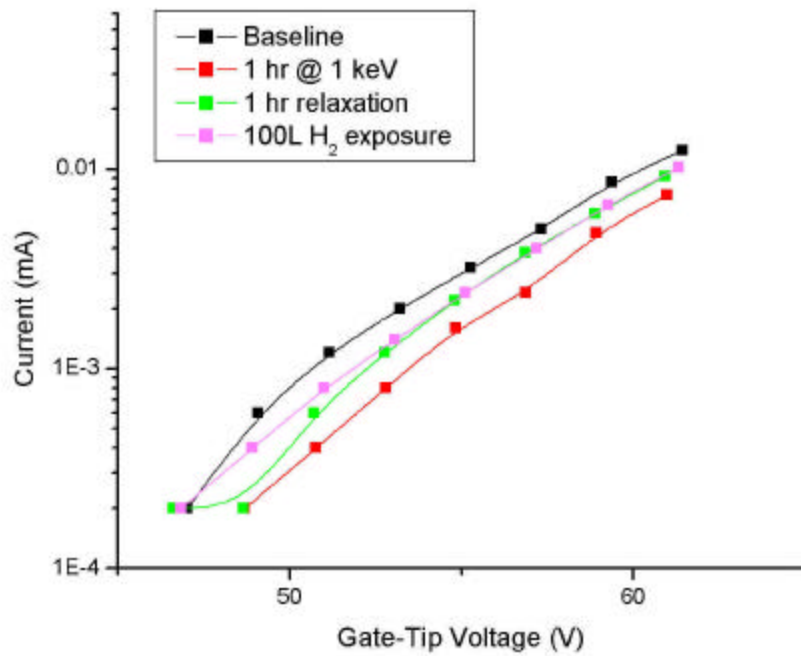


FIG. 11b. Hydrogen cleaning & exposure plot of Voltage versus Collector Current for  $\text{Ar}^+$  cleaning 1 keV (Logarithmic scale)

With the elimination of oxygen and hydrogen as potential candidates for the adsorbate species responsible for field emission improvement, study turned to other gases present in trace amounts within the system. Because field emission returns to baseline levels slowly over the course of several hours, it was postulated that this could be due to slow adsorption of trace gas(es) within the main chamber. Despite previously finding no measurable CH<sub>4</sub> resident in the main chamber, methane was chosen because others have suggested that methane dramatically increases emission for massive exposures (>1,000 L) [13-15]. For the exposures studied here, viz., on the order of tens or hundreds of Langmuir, methane was shown not to appreciably alter the field emission as displayed in figures 12. All trials tended to indicate that methane actually inhibited the slow progression to baseline levels after cumulative exposure larger than 300 L. Additional cleaning trials and time for relaxation resulted in field emission returning to pre-methane

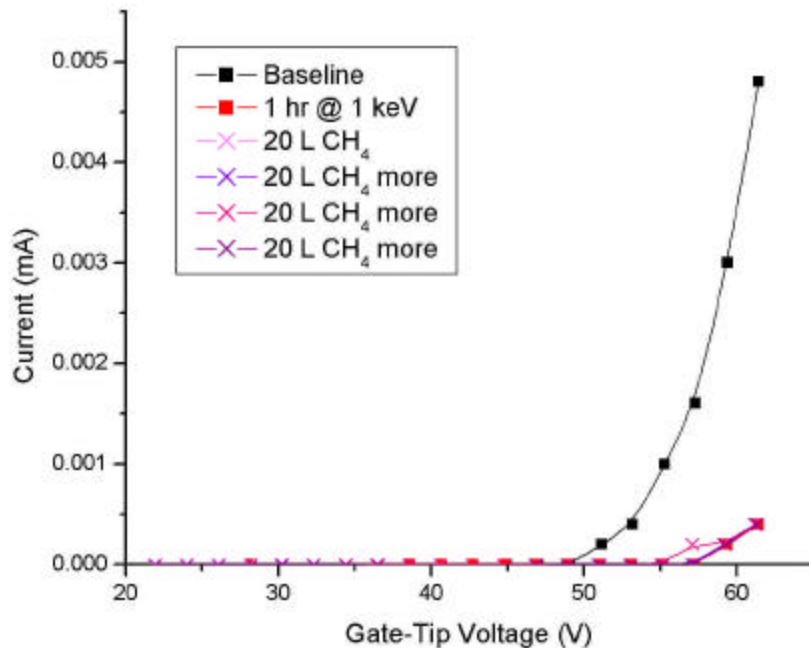


FIG. 12. Methane cleaning & exposure plot of Voltage versus Collector Current for Ar<sup>+</sup> cleaning 1 keV

baseline levels. This phenomenon could be due to the formation of carbon compounds on the surface of the molybdenum inhibiting emission until their removal.

Water was the last candidate for study because the adsorbate handling system had to be slightly modified for its exposure. This adsorbate presented additional complications when establishing pressure after exposure due to its affinity for metal surfaces like the inside of the vacuum chamber. Water was of particular interest because it was the principal contaminant in the system. Despite initial tests to the contrary, repeated trials revealed that water did not have an appreciable effect on the field emission for exposures up to one hundred Langmuir. As shown in Figures 13a and 13b, exposure to water after cleaning did not improve field emission.

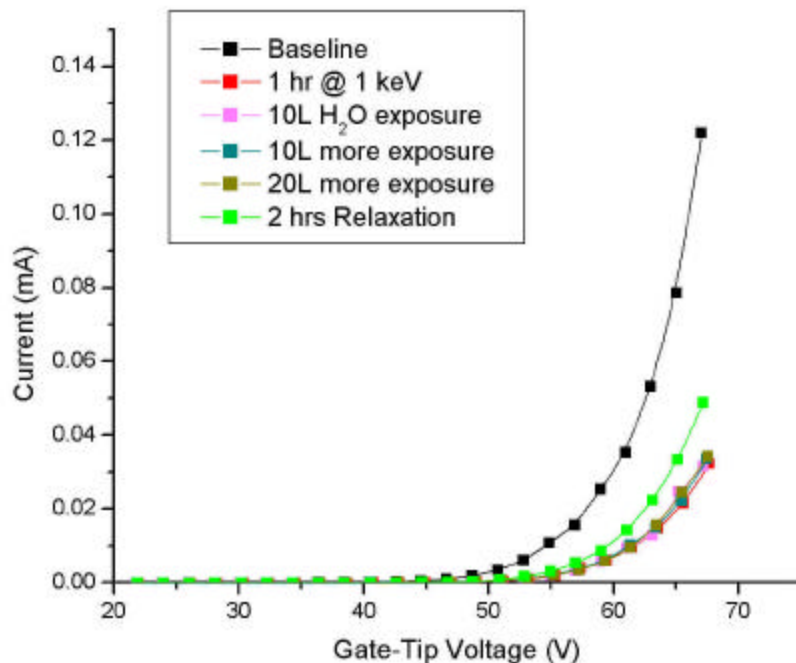


FIG. 13a. Water cleaning & exposure plot of Voltage versus Collector Current for Ar<sup>+</sup> cleaning 1 keV (Set 1)

Figure 13a shows cleaning and gradual exposure with some relaxation time (do nothing to the FEA) to show the natural progression back to baseline. Figure 13b shows cleaning and exposure after the relaxation trial.

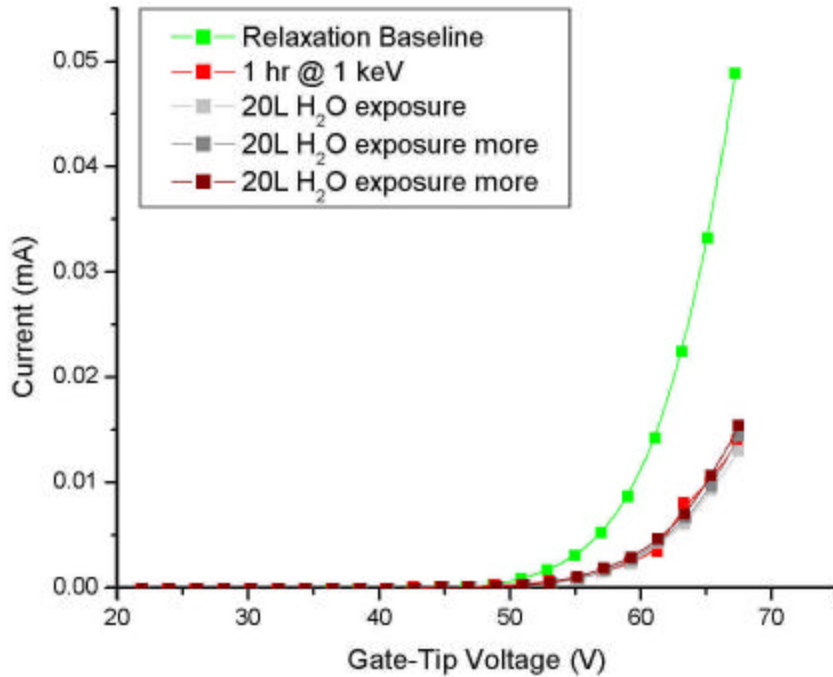


FIG. 13b. Water cleaning & exposure plot of Voltage versus Collector Current for Ar<sup>+</sup> cleaning 1 keV (Set 2)

## VII. Cathode Structure: General Comments Regarding Failure

Over the course of the investigation, four separate Spindt-type field emitter arrays were used. The first two FEAs were from a batch with 10,000 tips per cathode. The third and fourth FEAs had about 50,000 tips per cathode. All of the adsorbate trials discussed in the results were gathered using the fourth cathode. Despite the many precautions taken, three field emitter arrays were irreversibly damaged. These three cathodes were subsequently examined using a scanning electron microscope in an attempt to ascertain the nature of these failures. In November 2001, the first cathode was

subjected to a massive electrical discharge as the system rapidly lost vacuum pressure with operating voltages remaining between the gate and tips. A gate valve was inadvertently left open while stage two of the gas-handling system was filled at the same time a trial run was being taken. Figure 14 is a low-resolution picture of the cathode showing the catastrophic arc damage (the burned white portion) to the entire active surface and

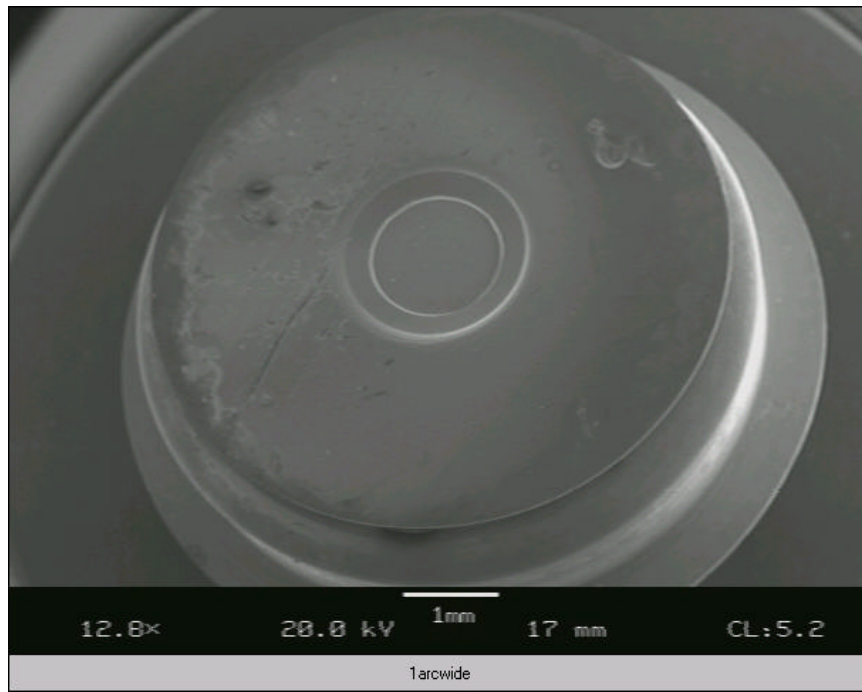


FIG. 14. Wide picture of first FEA and arc damage

surrounding mount. Figure 15 shows the extent of the damage to the active cathode surface where the gate and tips are normally visible. At this magnification, the tips should be clearly seen, instead only a grid of shadows is visible where the tips were melted from the surface. This incident was clearly preventable, and additional precautions were taken in future trials. The tips, gate, and collector were all grounded when the gas-handling system was changed and filled and when adsorbate was added to the main chamber.

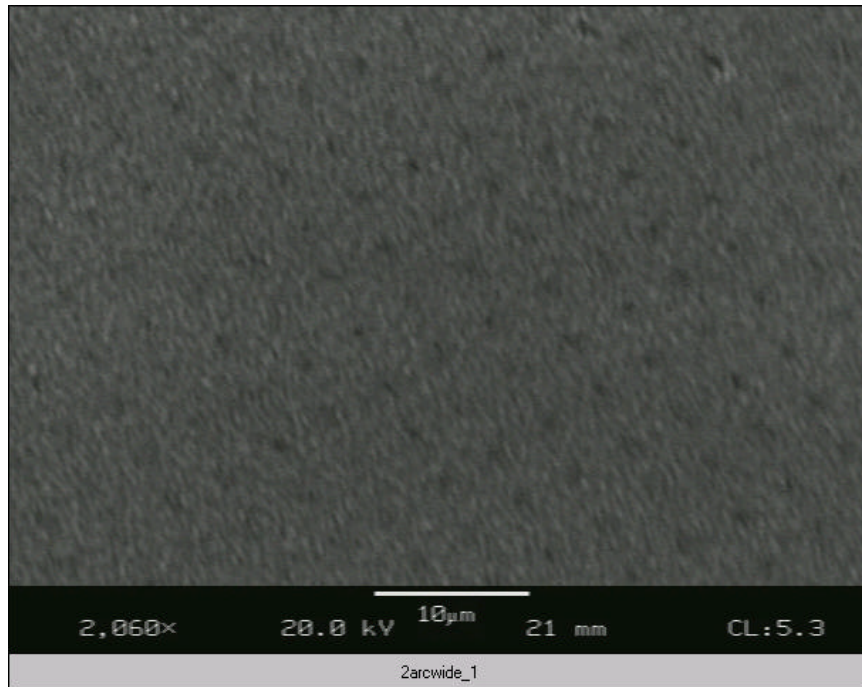


FIG. 15. Shadows of former tips on first FEA

The second FEA was damaged in early January under similar circumstances. During a field emission trial, the main chamber gradually lost pressure until an electrical discharge possibly damaged the cathode. However, there was no obvious source or reason for this failure. This was discovered when the field emitter failed to function correctly during trial runs. After the failure, the impedance between the gates and the tips was found to be on the order of a few megohms, while the impedance was previously measured to be greater than several tens of megohms when the cathode was placed into operation. The damage to the cathode was not immediately visible under the scanning electron microscope. Instead, the expected configuration of tips and gates was observed as in Figure 16. Some small debris on the active area were observed as well as small arc damage on the surrounding mount. Damage to the mount and fusing of tips and gates, possibly as a result of arc damage, have left this cathode ruined.

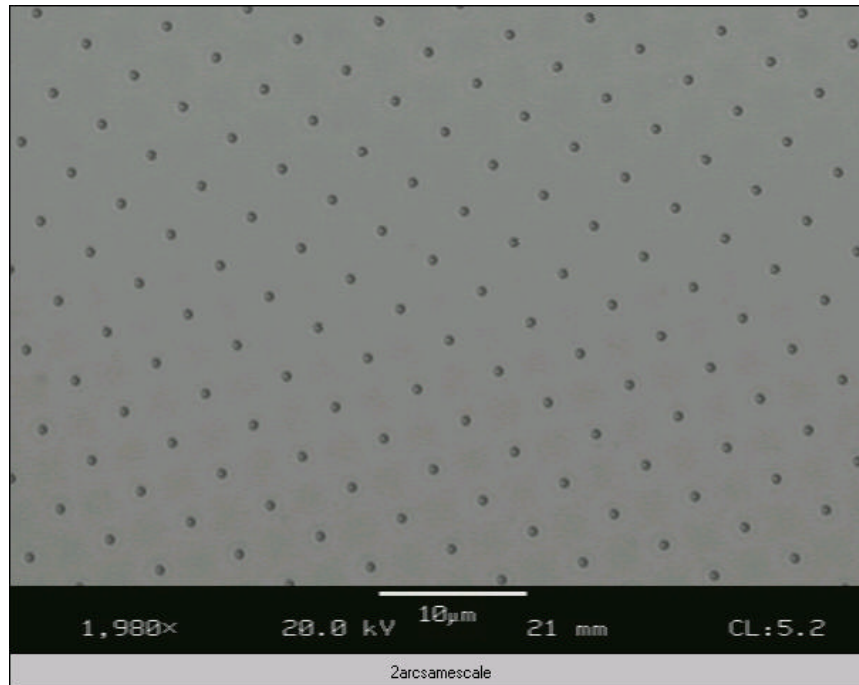


FIG. 16. Gates and tips on the second FEA

The third cathode enigmatically failed in March during normal operation. The failure did not correspond to any rapid change in pressure. Instead, the FEA failed after a series of cleaning trials in the middle of a subsequent I-V field emission measurement. The data collected immediately before and during failure are shown in figures 17a and 17b. At this point, four one-hour cleanings had taken place at ion energy of 1.125 keV. There was some concern that the current to the gate was too large in comparison to the current to the tips, but simple monitoring showed that this was clearly not the case. The cathode failed in the middle of an I-V measurement when the voltage was 47 volts, after the voltage measurement and before the collector current measurement. The failure resulted in the gate and tips being shorted, i.e., complete failure of the cathode. The impedance between the gate and tips was on the order of a hundred kilohms after the failure. When examined with the scanning electron microscope (SEM), catastrophic failure was clearly evident.

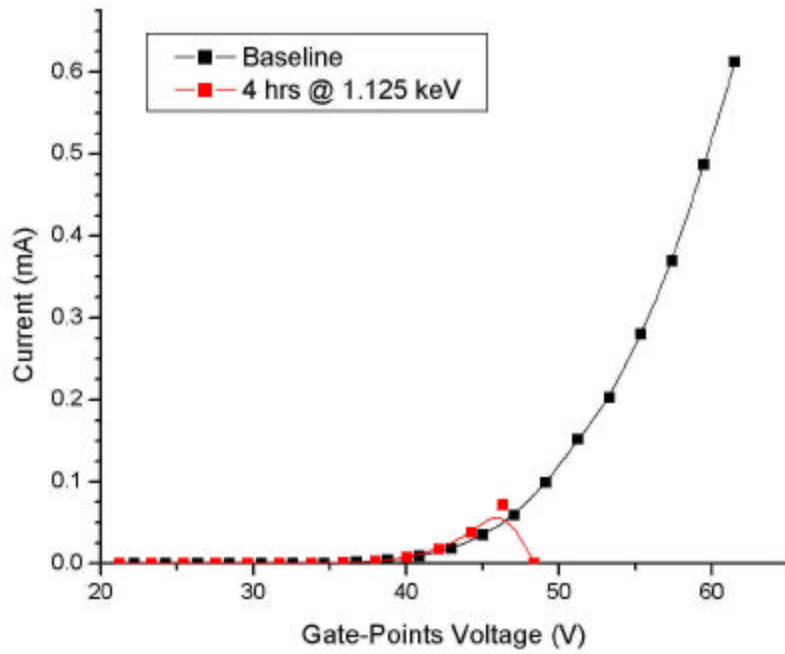


FIG. 17a. Failure plot of Voltage versus Collector Current for  $\text{Ar}^+$  cleaning 1.125 keV

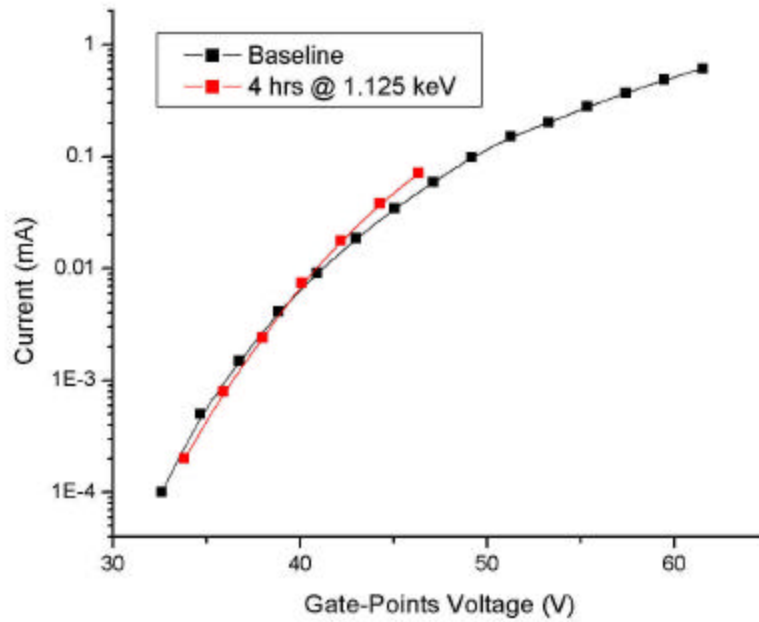


FIG. 17b. Failure plot of Voltage versus Collector Current for  $\text{Ar}^+$  cleaning 1 keV (Logarithmic scale)

Figure 18 shows a low-resolution picture of the cathode used in Figures 17a and 17b. The innermost circle is the active area of containing the gates and tips. At this magnification, what should have been a smooth, active area appears jagged and rough. In Figure 19, the active area appears to be seriously damaged. The portion with the tips seems to have accumulated foreign material in globules. The top layer of the surrounding ring appears to have either flaked off or accumulated some other substance. The damage to the outer ring can be seen in Figure 20. The gates can be seen in the upper left portion of Figure 20. Some of the gates in the lower portion have collapsed and formed a chasm, which was seen in other SEM pictures.

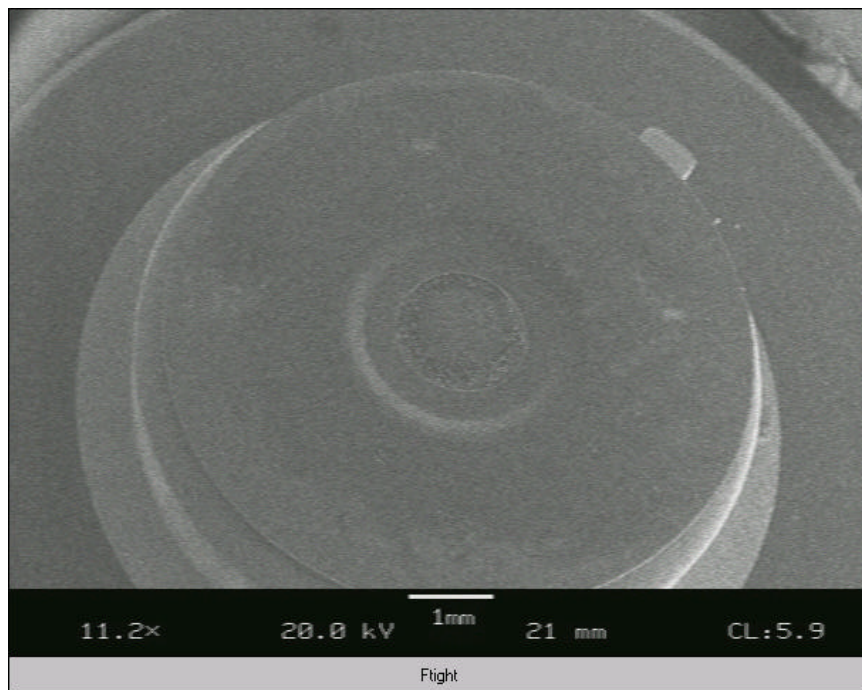


FIG. 18. Wide picture of the third FEA

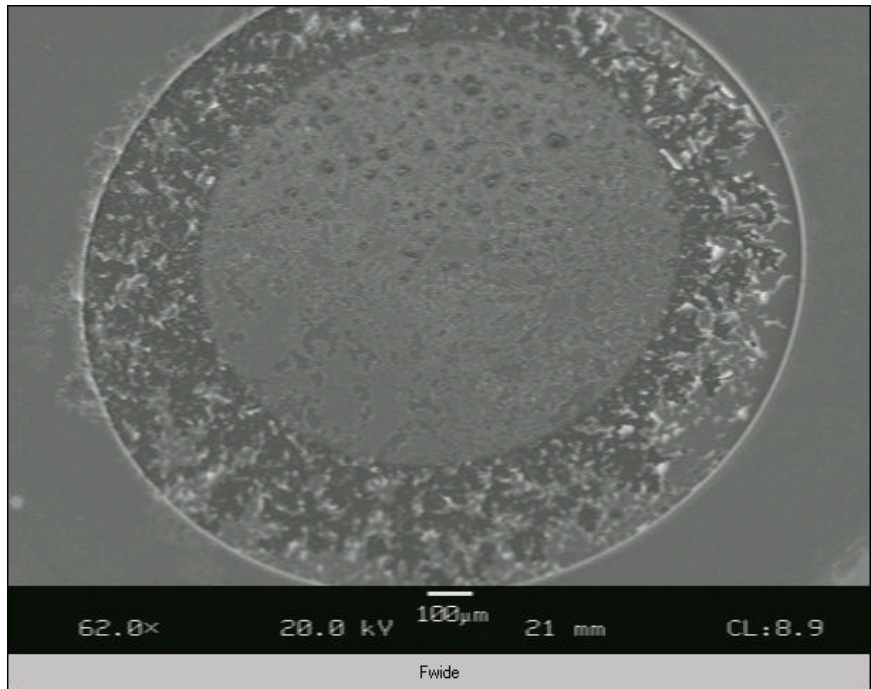


FIG. 19. Active area of the third FEA

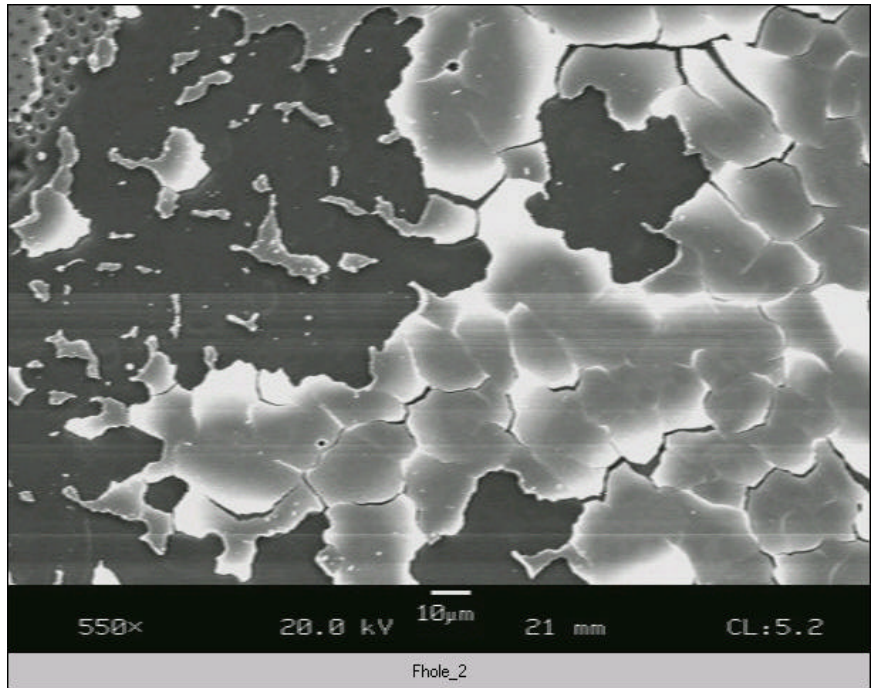


FIG. 20. Damage and ring surrounding active area

The damage to the gates and tips can be seen in Figure 21. Material seems to have accumulated on the surface of the gate structure. Some material has accumulated in large “globules,” which have deformed the gate structure.

To date, a satisfactory explanation has not been provided for what this material is and why it accumulated on the FEA. There appears to be too much material on the gate and surrounding structure to have come from explosion of the tips during the malfunction. Failure of the surrounding material may have been due to unexpected heating phenomena associated with the argon-ion cleaning beam. Relaxation time was allowed in between the cleaning trials and measurements of the field emission. Furthermore, earlier measurements immediately after cleaning and then periodically thereafter did not appear to show any appreciable change in field emission for several minutes after cleaning. If the cleaning was causing gradual damage to the field emitter due to temperature related phenomena, this should have been visible through baseline I-V

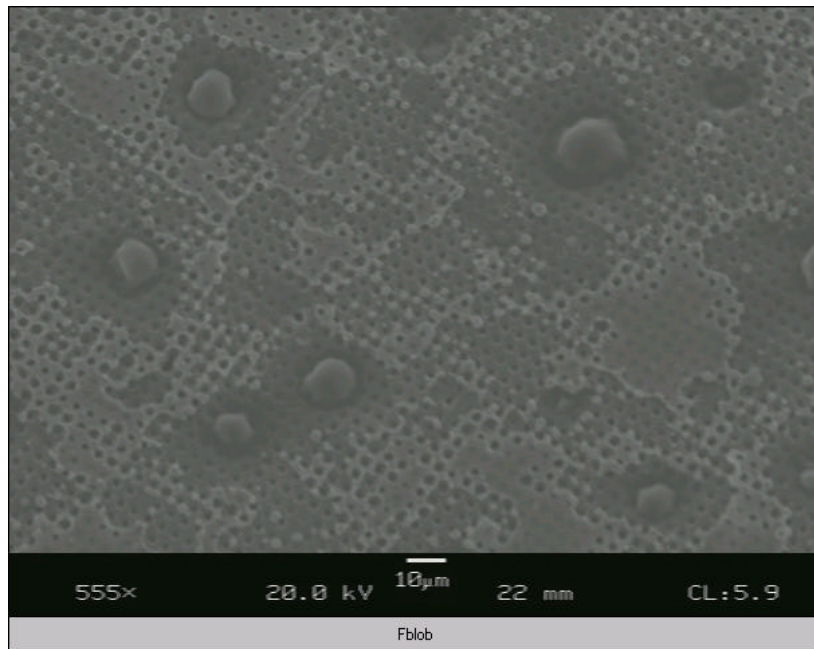


FIG. 21. Active area of the third FEA

measurements declining each day or changes in field emission soon after cleaning as the field emitter returns to normal temperature. Neither of these phenomena was observed. The material did not likely come from the burnout of any filaments because none failed during the trial or within several weeks. We are not aware of any protective coating on the FEA gate surface that was present to account for what appears to be extra material in the SEM picture.

## **VIII. Conclusions**

The goal of this investigation was to determine if the presence (or absence) of specific adsorbates could alter the field emission properties of molybdenum Spindt-type field emitter arrays as postulated in previous research. First, it was shown that argon ion bombardment at an energy of 1 keV for one hour consistently reduced field emission. The emission then returned to baseline levels within twenty-four hours. Presumably the  $\text{Ar}^+$  bombardment removed adsorbed atoms/molecules from the FEA. Gradual adsorption from background adsorbate levels in the main chamber could account for this return-to-baseline behavior. Since the field emission always returned to the previous day's baseline levels, it is unlikely that the cleaning process damaged the FEA.

In order to determine the identity of the adsorbate(s) associated with increased field emission, specific adsorbates were introduced to a cleaned FEA and field emission was monitored after each exposure. Oxygen, hydrogen, methane, and water were not observed to increase field emission upon exposure to a clean FEA for exposures of 10L up to several hundred Langmuir. Exposure to molecular oxygen immediately decreased field emission, which returned to previous levels after several minutes. With the

exception of carbon dioxide (CO<sub>2</sub>), all trace gases in the main chamber were used to expose a sputter-cleaned FEA in a controlled vacuum. If any of the tested adsorbates were responsible for the gradual increase in field emission, a dramatic field emission increase would have been observed under the exposure conditions of this experiment. Since that behavior was not observed, it must be concluded that trace amounts of these adsorbates in the main chamber were not responsible for the gradual increase in field emission observed after the FEA had been subjected to the Ar<sup>+</sup> ion beam.

Analysis of the data revealed that throughout cleaning and exposure, the Fowler-Nordheim relationship essentially described the measured I-V curve. Figure 22 depicts a typical Fowler-Nordheim plot for a cleaning and exposure trial. The data in Figure 22 are from the same trial as Figure 13a.

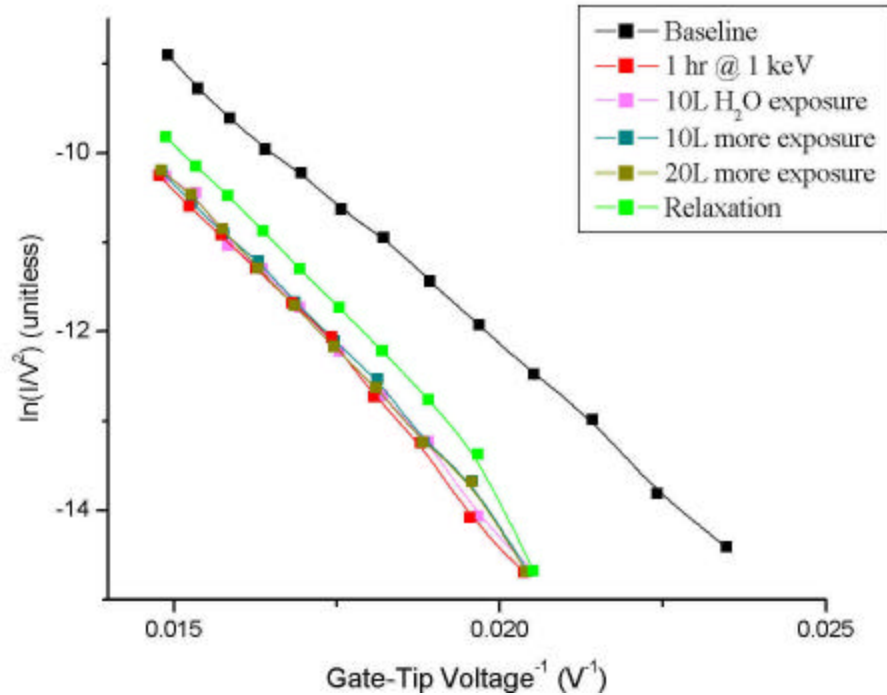


FIG. 22. Fowler-Nordheim plot for H<sub>2</sub>O exposure (Set 1)

What then is happening to the surface as a result of the ion bombardment that could account for this decrease and return-to-baseline behavior? The argon-ion beam at an energy of 1 keV could induce defects in the molybdenum surface or cause the MoO surface morphology to change. Such defects or alterations could relax over the course of several hours as the molybdenum surface returns to an equilibrium configuration. The adsorbates used in this experiment do not appear to affect this process except to hinder the progression in the short-term in the case of oxygen. One potential area for future study would be to examine whether the thermal environment of the cathode affects the field emission recovery rate after cleaning. Heating the cathode after cleaning may have an observable effect on the gradual reconstruction of the surface resulting in measurable changes of field emission (presumably shortening relaxation times).

This experiment could be performed with the usual cleaning procedure followed by a heating trial. In the heating trial, an intense beam of light such as a laser or a powerful halogen lamp could be focused on the cathode through the window in the main chamber for a period of time. Other heating sources could be used, such as heating strips on the entire main chamber, but the temperature change would only be on the order of a few tens of degrees Celsius. Furthermore, a drawback of heating the entire chamber is that the entire chamber would have to cool to room temperature before I-V measurements could proceed. When heating with a light source, the cathode must be rotated toward the viewing window, using a degree of freedom present in the armature but not used in the earlier adsorbate trials. After heating, the cathode would be allowed to cool to ambient temperature to eliminate simple thermal effects on emission and then perform the usual I-V measurements as before.

## **IX. Acknowledgements**

The author would like to extend his sincere appreciation to his advisor, Dr. Roy Champion, and to Wendy Vogan and Aidan Kelleher, whose input and technical assistance formed an integral part of this thesis. Special thanks go to Dr. Dennis Manos, Dr. Keith Griffioen, and Dr. James Smith for their service and input as my examining committee.

## X. References

- [1] C. A. Spindt, I. Brodie, L. Humphrey, E. R. Westerberg, *J. Appl. Phys.* **27** (1976) 5248.
- [2] R. H. Fowler, F.R.S., L. Nordheim, *Proc. Roy. Soc. London* **A119** (1928) 173.
- [3] T. S. Fahlen, *SPIE Proc.* **3636** (1999) 124 – 130.
- [4] I. Brodie, *Int'l J. Electron.* **38** (1975) 541.
- [5] A. H. W. Beck, *Proc. IEEE.* **106B** (1959) 372.
- [6] W. W. Dolan and W. P. Dyke, *Phys. Rev.* **95** (1954) 327.
- [7] A. van Oostrom, *J. Appl. Phys.* **33** (1962) 2917 – 2922.
- [8] J. M. Houston, *Phys. Rev.* **88** (1952) 349.
- [9] R. E. Burgess, H. Kroemer, J. M. Houston, *Phys. Rev.* **90** (1953) 515.
- [10] J. C. Tucek, S. G. Walton, R. L. Champion, *Surf. Sci.* **410** (1998) 258 – 269.
- [11] R. Riwan, C. Guillot, J. Paigne, *Surf. Sci.* **47** (1975) 183.
- [12] H. Xu, K. Y. Simon Ng, *Surf. Sci.* **356** (1996) 19.
- [13] B. R. Chalamala, R. M. Wallace, B. E. Gnade, “Residual Gas Effects on the Emission Characteristics of Active Mo Field Emission Cathode Arrays” Study for Flat Panel Display Division of Texas Instruments, Inc. (1998).
- [14] S. Itoh, T. Hiiyama, M. Yokoyama, *J. Vac. Sci. Technol. B.* **11** (1993) 647-650.
- [15] Babu R. Chalamala, Robert M. Wallace, Bruce E. Gnade, *J. Vac. Sci. Technol. B.* **16** (1998) 2855-2858.
- [16] Babu R. Chalamala, Robert M. Wallace, Bruce E. Gnade, *J. Vac. Sci. Technol. B.* **16** (1998) 2859-2865.
- [17] Babu R. Chalamala, Robert M. Wallace, Bruce E. Gnade, *J. Vac. Sci. Technol. B.* **16** (1998) 2866-2869.
- [18] J. W. Gadzuk and E. W. Plummer, *Rev. Mod. Phys.* **45** (1973) 487 – 548.